Journal of Applied Biological Sciences
E-ISSN: 2146-0108 17(2): 328-341, 2023
DOI: https://doi.org/10.71336/jabs.957
Research Article

SPECTROSCOPIC STUDIES ON THE INTERACTION BETWEEN THE HUMAN HEMOGLOBIN WITH FOOD ADDITIVE AMARANTH NANOPARTICLE USING BINDING SITES AND MOLECULAR DOCKING

S. Bakkialakshmi*, S. Chithra

Annamalai University, Department of Physics, Annamalai Nagar, Tamilnadu, India

**Corresponding Author:*
E-mail: bakkialakshmis@rocketmail.com

(Received 10th June 2021; accepted 17th May 2023)

ABSTRACT. The human hemoglobin (HHb) interaction analysis with the Amaranth nanoparticle system (Amt-NS) was investigated using UV-VIS spectrophotometric and spectrofluorimetric techniques, such as synchronous fluorescence, steady state fluorescence, Forster resonance energy transfer (FRET) and time-resolved fluorescence. Amaranth nanoparticle system (Amt-NS) was prepared by ionic gelation method and characterised by particle size analyser, Fourier transform infrared (FTIR) and scanning electron microscope (SEM) analyses. An intimate binding interaction between the Amt-NS (food colourant) and HHb protein was predicted in this study. The findings revealed that Amt-NS altered the environment of tryptophan and tyrosine residues in HHb. The analysis of synchronous fluorescence and time resolved fluorescence confirmed the fluorescence quenching process. There was an estimate of the binding constant and number of binding sites. Molecular docking and antibacterial activity have been studied. The experimental findings of fluorescence were in line with the results obtained from studying molecular docking. The molecular docking experiment revealed the binding mode of the complex of HHb and Amt-NS.

Keywords: *Amaranth nanoparticles, antibacterial activity, fluorescence, human hemoglobin, molecular docking.*

INTRODUCTION

Nanotechnology has a significant effect on medicine. Proteins absorb to their surface as a nanoparticle approaches the biological medium [1, 2], contributing to protein corona formation. Indeed, high surface-to-volume ratios of nanoparticles contribute to the protein binding [3, 4] of their large surface area, as well as the adsorption and trapping of a substantial number of proteins on the surfaces of nanoparticles [5]. In nanomedicines and nanotoxicology, interaction of nanoparticles with proteins has recently been considered to be important. Nanoparticles in the body can interfere with proteins and can have significant effects on the structure and function of the protein [6, 7].

Food colourants, in general, are natural or synthetic dyes or pigments used to enhance the appearance of foods. Amaranth (C.I Food Red 9, E123, FD&C Red No.2) (Fig.1) is a reddish or brownish colour that is commonly used to portray several foodstuffs in the

food industry [8, 9]. It is identified that amaranth (Amt) is possibly toxic to in vitro human lymphocytes [9]. The positive genotoxic effects of amaranth have also been demonstrated in an in vitro chromosomal aberration assay [10]. It may also induce asthmatic and allergic reactions when certain susceptible individuals come into contact with certain medications, such as aspirin, within the body [11, 12]. Given all of the potentially detrimental health implications of amaranth, it's an essential necessity to check the intake of this synthetic colour.

Hemoglobin (Hb) is an iron-containing protein present in the red blood cells of vertebrates. The high-resolution atomic structure of human hemoglobin (HHb) revealed that it is tetrameric, with two identical α-chains and two identical β-chains having 141 and 146 amino acid residues [13, 14]. There are seven and eight helices respectively in these α and β-chains. The essential to its biochemical functions is the tetrameric confirmation of HHb. The delivery of oxygen and carbon dioxide to all parts and organs of the body, the regulation of blood pH, and the movement of electrons are all functions of Hb. By interacting with them, HHb may also affect the delivery, metabolism and toxic activity of several small molecules [15, 16, 17]. Therefore, observing the interaction of small molecules with HHb is crucial. While the interaction of colourants was barely investigated [18, 19]. Therefore, the influence of amaranth nanoparticle system (Amt-NS) food colourant on HHb using spectroscopic techniques will be studied in the present study.

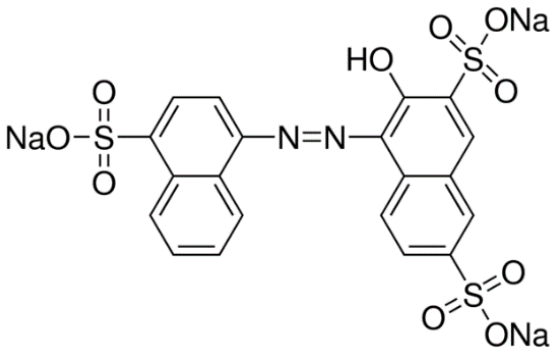

Fig.1. *Molecular structure of amaranth*

MATERIALS AND METHODS

Materials

Human hemoglobin and amaranth were purchased from Sigma-Aldrich Bangalore, India. Low molecular weight Chitosan (CS) and Sodium tripolyphosphate were purchased from Sisco research laboratory Chennai, India.

Preparation of Amt-NS

Amt-NS, modified ionic gelation was carried out as described [20, 21], in which chitosan polycation groups engage with a polyanionic tripolyphosphate (TPP). The amaranth solution was poured into a Chitosan solution (0.6% w/v) made by dissolving chitosan in dilute acetic acid (1% v/v) at room temperature. TPP, dissolved at 5mg/ml (w/v) in de-ionized water, was immediately applied to the emulsion dropwise [21]. The

dropwise addition of TPP solution rapidly produced the nanoparticles that had been magnetically agitated (100 rpm) at room temperature. The CS/TPP ratio for the construction of the nanoparticle system in the formulations was held at 3:1 (w/v). The resultant colloidal assembly system, i.e., the nanoparticle system's composition, was agitated continuously for 30 minutes, and the products were centrifuged for 15 minutes at 2.000 rpm, then washed with filtered de-ionized water to remove the ethanol.

Characterization of amaranth nanoparticles system (Amt-NS)

By the particle size analyser, the particle size was determined (Micrometrics CPE-11 Nano plus). Furthermore, the scanning electron microscope is used to determine the morphological characteristics of the nanoparticles (JEOL-JSM-IT 200). And X-Ray Diffractometer (XRD) evaluated the XRD for Amt-NS (BRUCKER D8 Advance). The Amt-NS and amaranth powder Fourier transform infrared (FTIR) spectra were analysed by FTIR spectroscopy (AGILENT CARY 630 FTIR Spectrometer) Annamalai University, India.

Spectroscopic instruments details

Absorption spectral studies were recorded using UV/Visible spectrophotometer (Shimadzu 1800 pc UV/Visible spectrophotometer), Annamalai University, India. Steady state fluorescence measurements were performed on Shimadzu RF-5301 PC (Shimadzu corporation, Kyoto, Japan). Fluorescence decay measurements were recorded using Hariba-Jobin Yvon [spex-sf B-III] spectrofluorimeter.

Molecular docking study

The protein data bank (PDB) has acquired the HHb crystal structure used for molecular docking (PDB ID: 1BZ1). The Avogadro 1.1.1 molecular editor was used to lower the energy structures of AO and 9AA. PyMOL software was used to remove water molecules and all associated ligand molecules except heme groups from HHb's downloaded PDB crystal structure. Polar hydrogen atoms and gasteiger charges were added to the HHb crystal structure before the docking procedure began. The Lamarckian Genetic Algorithm (LGA) was used to dock proteins and ligands in the AutoDock 1.5.6 application. The autodock and PyMOL applications were used to assess the output.

Antibacterial activity using Agar well diffusion method

The antimicrobial activity of mucus extracts was tested using the agar well diffusion method using Muller Hinton agar (MHA) Annamalai University, India, as the antibacterial medium. Bacterial and fungal inoculums have been prepared from a 24-hour culture colony on a nutrient broth medium. The inoculum was calibrated with McFarland density to achieve a final construction of between 10^4 & 10^6 CFU /mL for the bacteria. 50µg of each extract was infused onto Whatmann AA filter paper and put to test medium that had already been infected with each test strain. At 37 °C, bacteria plates were incubated. After a 24-hour incubation period, inhibition zones were measured [22].

RESULTS AND DISCUSSION

Characterization of amaranth nanoparticles (Amt-NS)

UV-Visible spectroscopy

The primary technique for analysing the size and shape of nanoparticles is UV-Visible spectrometry. As these nanoparticles exhibit an extreme peak of absorption due to the excitation of the surface plasmon, it is very susceptible to the presence of colloids. UV-Visible spectral analysis was done using Shimadzu 1800 PC UV/Visible spectrophotometer. A tiny aliquot was drawn from the reaction mixture and a spectrum was taken from 200 nm to 800 nm on a wavelength. UV/Visible results show the standard absorption peak of Amt-NS at 270 as expressed in Fig.2.

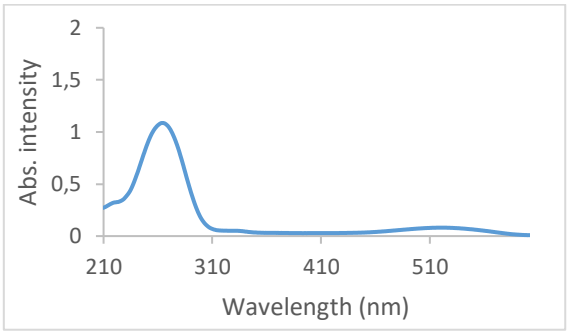

Fig 2. *UV/Vis absorption spectra of Amt-NS*

Particle size analyser

A particle size analyser was used to obtain the particle size. At 25 ^{o}C temperature, the observation was performed with water as the solvent. As a consequence of the observation, Amt-NS formulations have an average particle size of 260.9 nm (Fig.3). Particles obtained have, as specific, a nanometer size range. Colloid nanoparticle as several advantageous properties, including that nano-size steadily makes it much more stable to sediment. The index of polydispersibility observed from the particle size analysis was -0.072. the polydispersibility index defines the distribution of the particle sizes found in the preparation of nanoparticles, the lower the polydispersibility index, the more uniform the particle sizes and where there is a substantial variation in size between the larger and smaller particles, the characteristic of the particles will be influenced. The greater the particle size, the simpler it is to settle the particle [23].

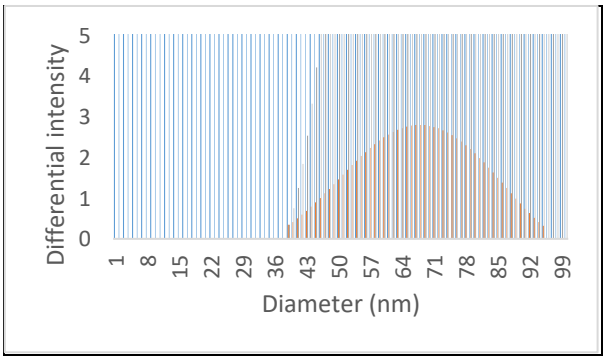

Fig.3. *Particle size analysis of Amt-NS*

Scanning electron microscopy (SEM)

SEM microscopy has been used to evaluate the morphology of nanoparticles on the surface. SEM images were obtained at varying magnification. A narrow, highly concentrated beam of electrons is swept over a tiny sample, and the electrons passing through the thin sample are captured on a detector situated under the sample, resulting in the desired brilliant filled pictures. SEM will permit us to provide a more detailed prediction of the distribution of nanoparticles by size. A unique nanoparticle from with a diameter range of 50-450 nm was seen in Fig.4. The transmitter electrons are being directed by an electron multiplier, i.e., a gold plate, on to a traditional detector.

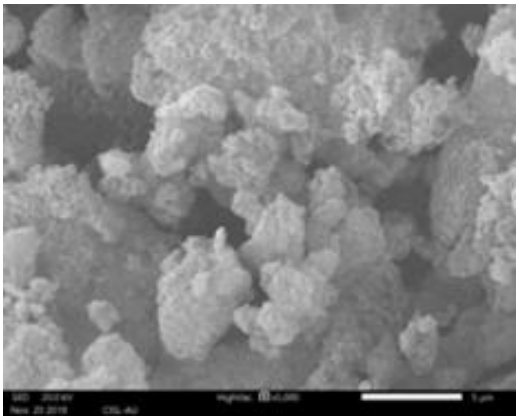

Fig.4. *SEM image of Amaranth nanoparticles*

XRD analysis

An X-Ray diffractometer was used to estimate the crystalline state of the samples. The Amt-NS XRD patterns at flow rate (8 and 10 ml/min) and the sample revealed the presence of several different peaks at 2θ (22.79), incanting that the Amt-NS are of a crystalline form as the findings are seen in Fig.5.

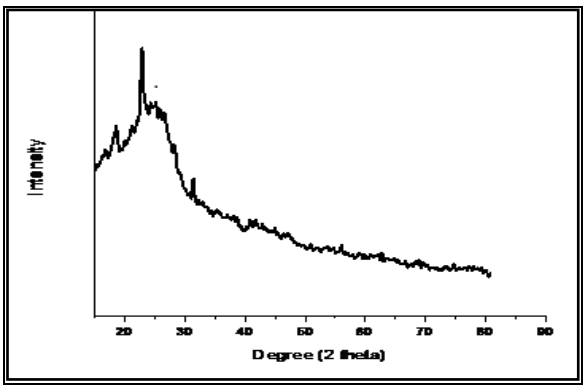

Fig.5. *X-Ray diffraction pattern of Amaranth nanoparticles*

FTIR studies

In order to find out the structural modification of Amt food colourant after being converted into nanoparticles, FTIR measurements were carried out. The analysis of the Amt-NS peaks has been replicated in the Amt-NS FTIR spectrum and there is no

significant change in the Amt-NS spectrum (Fig.6). Probable measures of C-O and C-OH vibrations are the usual peak at 1166 cm^{-1} [24] and another peak at 1286 cm^{-1} due to C-O stretching [25]. There is also a 1619 cm^{-1} peak that may be assigned to the stretching of C=O and C-N. the spectrum shows a broad bond in hydroxy groups and phenols and alcohols at 3365 cm^{-1} that corresponds to O-H stretching and also confirms the existence of NH_2 groups.

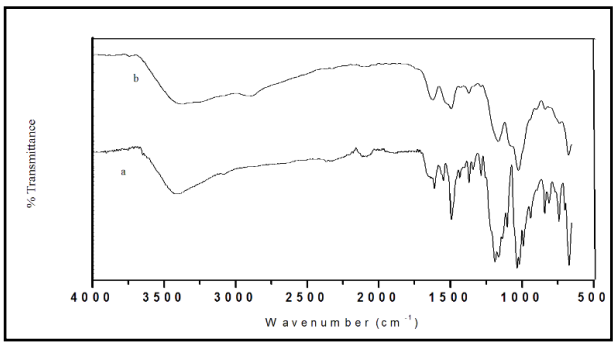

Fig.6. *FTIR spectra of a) Amaranth b) Amaranth nanoparticles*

Absorption spectral study of HHb with Amt-NS

Hemoglobin has a distinct absorption spectrum between 190 and 450 nm, with two well-defined peaks located at 202 and 405 nm, respectively. In 190-450nm range, the interaction of Amt-NS with HHb was recorded. As incremental quantities of Amt-NS are added, the absorption spectra of hemoglobin changes, as seen in Fig.7. Peak at 406nm had roughly 14% hypochromicity after binding with the Amt-NS. In terms of intimate interaction between the Amt-NS and the HHb, certain spectral changes can be perceived. The peak's location remained constant in the presence of Amt-NS. The spectrophotometric data was analysed by graphing the reciprocal of the absorbance difference with respect to the reciprocal of the Amt-NS concentration. Bensi-intercept Hildebrand's to slope ratio [26] was calculated, and the value was calculated as K_g (1.2 M^{-1}).

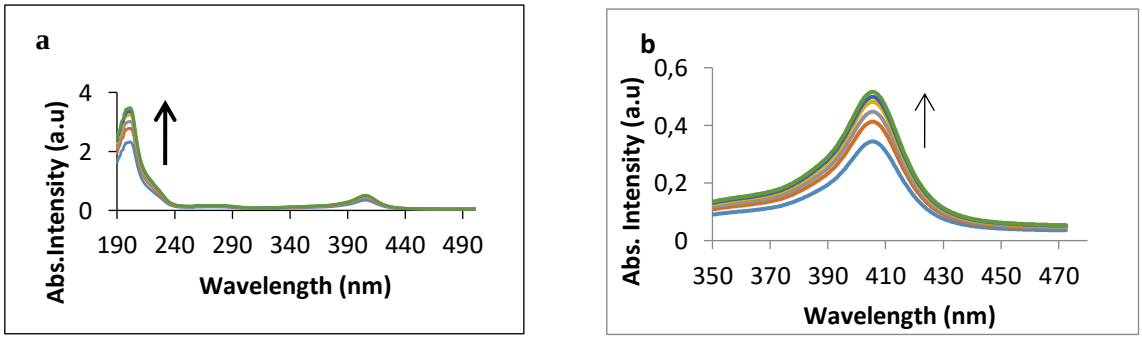

Fig. 7. (a) *UV-VIS absorption spectra of HHb with different concentrations Amt-NS (mol L^{-1}) (1) 0.0, (2) 0.2, (3) 0.4, (4) 0.6, (5) 0.8, (6) 1.0.* ***(b)*** *The 405 nm band is highlighted.*

Fluorescence spectral study

Fluorescence spectroscopy is one of the most extensively used technique for studying the interaction between ligands and proteins. The tryptophans, tyrosines and phenylalanines are the intrinsic fluorophores in Hb. There are six tryptophan (Trp) residues in total three Trp residues in each of the two αβ – dimers α-Trp14, β – Trp 15 and β – Trp 37 [27], and five tyrosine residues in each of the αβ-dimers α-Tyr24, α-Tyr42, α-Tyr140, β - Tyr34 and β – Tyr 144 [28]. The β-Trp 37 residue at the α1β2 interface is thought to be primarily responsible for the intrinsic fluorescence of the HHb molecule [29]. As a result, when Amt-NS is introduced, analysing variations in the intrinsic fluorescence of HHb can provide insight into the environmental alterations around the Trp37 moiety. At 330nm on excitation at 280nm, HHb has strong fluorescence emission peak shown in Fig.8. The fluorescence of HHb was very effectively quenched by the Amt-NS. Using the Stern-Volmer equation, the details after the inner filter effect correction was evaluated.

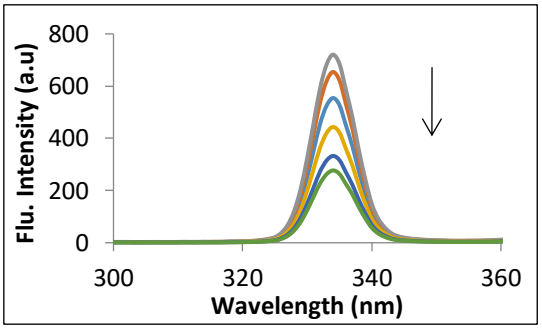

Fig. 8. *Steady–state fluorescence spectra of HHb with different concentrations of Amt- NS (mol L^{-1}) (1) 0.0, (2) 0.2, (3) 0.4, (4) 0.6, (5) 0.8, (6) 1.0.*

Spectral studies were carried out to explicate the quenching mechanism in the association of Amt-NS with HHb fluorescence. The process was clarified using the Stern-Volmer equation (1) [30].

$$F_0/F=1+K_q\tau_o[Q]=1+K_{sv}[Q] \qquad (1)$$

Here, the presence and absence of the quencher, F and F_o are the fluorescence intensities, K_q is the quenching rate constant and is equal to the K_{sv}/τ_o, K_{sv} is the quenching constant of Stern – Volmer, τ_o is the protein's average lifetime in the absence of the quencher and [Q] is the quencher's concentration, respectively. K_{sv} and K_q values are listed in Table 1. And Fig.9 shows the Stern - Volmer graphs of the Amt-NS quenching of the fluorescence of HHb tryptophan residues. It shows that the Stern-Volmer graphs are linear, demonstrating the presence of just one form of quenching, either static or dynamic.

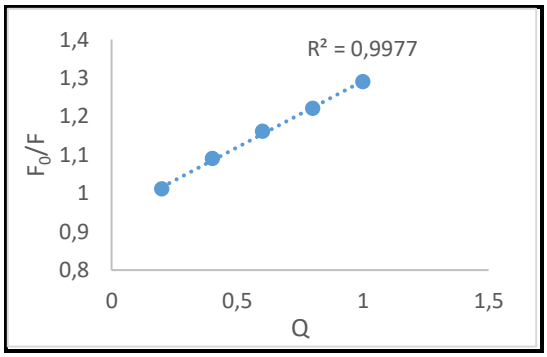

Fig.9. *Stern-Volmer plot for the quenching of HHb by Amt-NS concentrations*

Fluorescence Lifetime Study

Fluorescence quenching, according to the Lakowicz hypothesis, may effectively discriminate between dynamic and static processes using time-resolved fluorescence measurements [31]. Static quenching illustrates the same fluorescence lifetime values, while dynamic quenching represents significant changes in fluorescence lifetime values [31]. In the absence and presence of Amt-NS, time-resolved fluorescence lifetime measurements were performed for HHb, as shown in Fig.10. The time-resolved fluorescence decay curves of free and complex HHb were used to compute their fluorescence lifetime values and corresponding amplitudes. Here, τ=fluorescence lifetime and α= relative amplitude. For free HHb, the fluorescence lifetime values were τ_1=2.55ns and τ_2=7.53ns. The average fluorescence lifetime values were determined to be τ_1=1.97ns and τ_2=6.97ns after the addition of Amt-NS, respectively. Because the Trp residues contain many exponential decays, the overall lifetime of fluorescence was employed to derive qualitative insights rather than individual components. The mean fluorescence lifetime of free HHb was 3.76ns, although it was slightly altered to 2.36ns in the presence of Amt-NS. As a result, the fluorescence lifetime of free HHb remained nearly unaffected in the presence of Amt-NS. This result confirmed that the quenching process is primarily static and due to HHb and Amt-NS complexity.

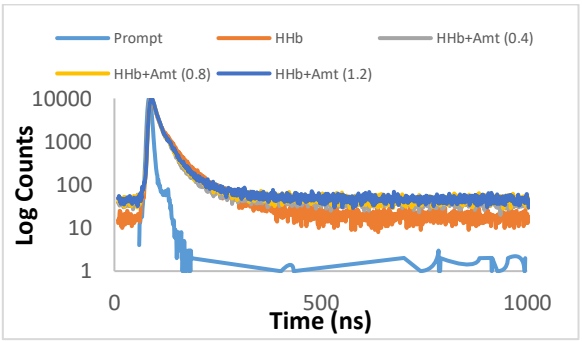

Fig. 10. *Time – resolved fluorescence spectra of HHb with different concentrations of Amt-NS (mol L^{-1}) (1)0.0, (2)0.4, (3)0.8, (4)1.2.*

Binding model and Binding sites

Because the fluorescence quenching of HHb by Amt-NS was a static quenching process, the apparent binding constant (K_a) and the number of binding sites (n) may be calculated using the following equation [32].

$$\text{Log } (F_o\text{-}F)/F = \text{Log } K_a + n \text{ Log } [Q] \qquad (2)$$

Where Ka was the binding constant and n the number of binding sites, the number of Amt-NS bound to the HHb macromolecule was calculated. The values of K_a and n were calculated by plotting Log $[(F_o\text{-}F)/F]$ vs Log [Q], with n as the slope and log Ka as the intercept on the Y-axis (Fig.11). For the Amt-NS – HHb system, the binding constants K_a and binding sites n were shown in Table 1. With the site - binding model Eq. (2), the interaction between Amt-NS and HHb agrees well. The presence of a single binding site for Amt-NS in HHb was indicated by n values of around 1.

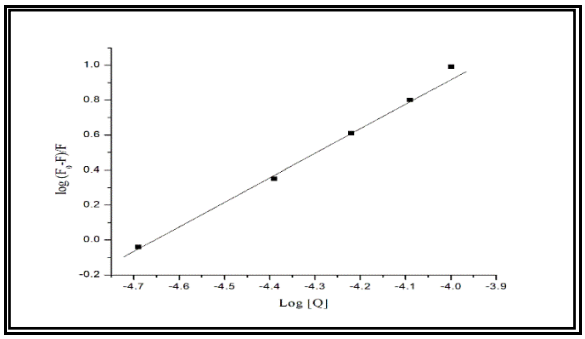

Fig.11. *The plot of log (F_0-F)/F versus log (Q) HHb with Amt-NS*

Table 1. *Stern–Volmer (K_{SV}) and bimolecular quenching rate constant (K_q), binding constant (K_a) and binding site (n) of HHb with Amt-NS*

Quenchers	K_{SV} x 10^5 (L mol^{-1})	K_q ($Lmol^{-1}$ S^{-1}) x 10^8	K_a x10^5 (L mol^{-1})	n
Amaranth - NP	1.45	3.85	1.98	1.37

Synchronous fluorescence study

The amount of confirmational alterations in the protein following amaranth binding has been investigated using synchronous fluorescence experiments [33]. When the scanning distance is fixed between the excitation and emission wavelengths of 15 and 60nm, respectively, the synchronous fluorescence of HHb is typical of tryptophan and tyrosine residues. The quenching by the Amt-NS of HHb fluorescence is then representative of a shift in the polarity around these residues [34]. The impact of Amt-NS at a wavelength of $\Delta\lambda$=60nm on the synchronous fluorescence of HHb revealed that the fluorescence steadily reduced as the maximum emission redshifted (Fig. 12a). This red shift suggests that in a hydrophobic environment, tryptophan residues are more accessible to solvent molecules. Interestingly, the emission maximum at $\Delta\lambda$=15nm does not vary at

all, indicating that there is very little change in the microenvironment impacting the tyrosine residues (Fig. 12b). Amaranth affected the polarity around β-Trp37, whereas the polarity surrounding tyrosines remained mostly unaltered, indicating that tryptophan residues were involved in the complexation process.

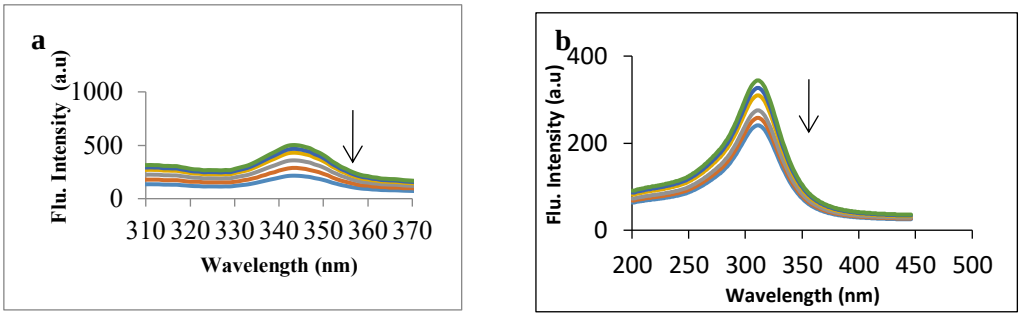

***Fig.12**. Synchronous Fluorescence Spectra for HHb with Amaranth - NS a) $\Delta\lambda$ = 60 nm and b) $\Delta\lambda$ = 15 nm*

Forster resonance energy transfer (FRET) study

Forster resonance energy transfer (FRET) is referred to be a "spectroscopic ruler" for estimating molecule distances in macromolecular systems [35]. Measurements of energy transfer efficiency can reveal the distance between the bound Amt-NS and its HHb interaction site, which is significant for understanding the structural and confirmational elements of the Amt-NS and HHb complex [36, 37]. The values of E and J (fluorescence emission spectrum integral overlap of HHb and the absorption spectrum of Amt-NS), R_o (50 percent energy transfer effectiveness critical distance) and r (HHb and Amt-NS distance) were deduced to be 39.9, $2.77x10^{-15}cm^3$ L mol^{-1}, 1.74nm and 2.82nm respectively [38]. As a result, the HHb fluorescence spectrum and the Amt-NS absorption spectrum have enough overlap (Fig.13). There's a good chance that energy will be transferred from HHb's Trp residue to Amt-NS [39]. HHb and Amt-NS are less than 8nm apart. From these observations we can unambiguously infer that the relation between Amt-NS and HHb arises from strong ground state complex.

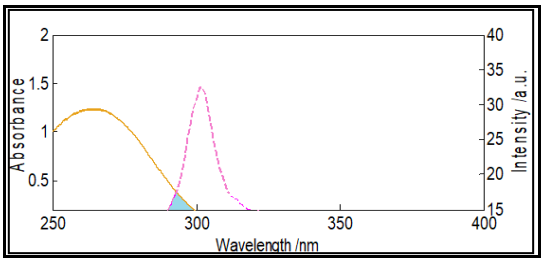

***Fig.13.** The overlap of UV absorption spectra of Amt – NS (solid line) with the fluorescence emission spectra of HHb (dotted line)*

Molecular docking study

Molecular docking experiments have been used to further demonstrate the binding and positioning of the Amt-NS on HHb. The impacts of the docking phase of the lowest energy confirmation chosen and amplified ligand site may be shown in Fig.14, displaying the small molecule's overall location on the HHb polypeptide chain. There are

hydrophobic rings in both AO and 9AA that can interact in the polypeptide chain with hydrophobic amino acid residues that from H-bonding interactions. AO establishes one H-bonding contact with Arg-40, whereas 9AA creates three H-bonding connections in the polypeptide chain with Arg142, Thr138, and Asp 127 residues. In the vicinity of the Amt-NS molecules, the presence of hydrophobic residues indicates the presence of hydrophobic interaction between the HHb and the Amt-NS molecules.

Antibacterial activity

Using the agar well diffusion process, the antibacterial activity of Amt-NS and HHb was evaluated (Fig.15). The sample had responded to antibacterial activity, as seen on the plates. For antibacterial function testing, *E. coli*, Salmonella sp., and *Vibrio cholerae* (Gram-negative) and Staphylococcus sp., (Gram-negative) bacterial models were used. Amt-NS – HHb is an important antibacterial substance.

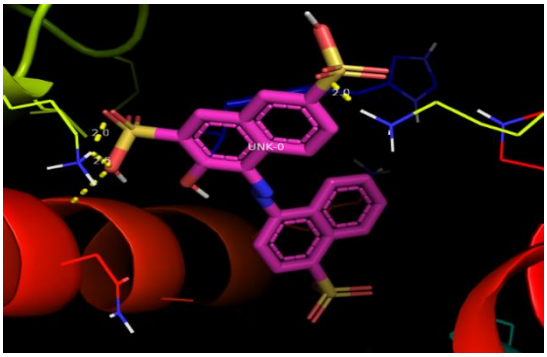

Fig.14. *Docking image of HHb with Amt-NS*

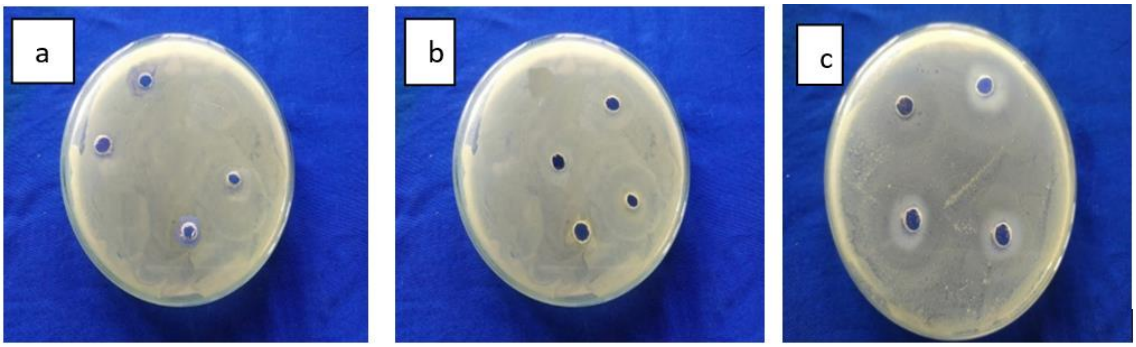

Fig. 15. *Antibacterial activity of a) Amt-NS b) HHb c) HHb with Amt-NS*

CONCLUSION

This study provides a detailed spectroscopy of the interaction between the food colourant amaranth nanoparticles system and human hemoglobin. Amt -NS efficiently depleted HHb fluorescence and considered the quenching mechanism to be static in nature. The analysis of synchronous fluorescence showed that polarity around Trp

residues were changed when Amt-NS was binding. Studies of molecular docking using Autodock also shown that Amt-NS bound HHb. However, for each food colorant several binding confirmations of very close energies were expected.

Conflict of Interest. The authors declared that there is no conflict of interest.

Authorship Contributions. Concept: S.B., S.C., Design: S.B., S.C., Data Collection or Processing: S.B., S.C., Analysis or Interpretation: S.B., S.C., Literature Search: S.B., S.C., Writing: S.B., S.C.

Financial Disclosure. This research received no grant from any funding agency/sector.

REFERENCES

[1] Walkey, C.D., Olsen, J.B., Guo, H., Emili, A., Chan, W.C.W. (2011): Nanoparticle size and surface chemistry determine serum protein adsorption and macrophage uptake. Am. Chem. Soc. 134: 2139–2147.

[2] Dell'Orco, D., Lundqvist, M., Oslakovic, C., ommy Cedervall T., Linse, S. (2010): Modeling the time evolution of the nanoparticle-protein corona in a body fluid. PLoS One 5: 1–8.

[3] Klein, J. (2007): Probing the interactions of proteins and nanoparticles. PNAS 104: 2029–2030.

[4] Lynch, I., Cedervall, T., Lundqvist, M., Cabaleiro-Lago, S., Dawson, K.A. (2007): The nanoparticle–protein complex as a biological entity; a complex fluids and surface science challenge for the 21st century. Adv. Colloid Interface Sci. 134:167–174.

[5] Boulos, S.P., Davis, T.A., Yang, J.A., Lohse, S.E., Alkilany, A.M., Holland, L.A., Murphy, C.J. (2013): Nanoparticle-protein interactions: a thermodynamic and kinetic study of the adsorption of bovine serum albumin to gold nanoparticle surfaces. Am. Chem. Soc. (Langmuir) 29: 14984–14996.

[6] Calzolaim, L., Franchini, F., Gilliland, D., Rossi, F., (2010): Protein-nanoparticle interaction: identification of the ubiquitin-gold nanoparticle interaction site. Nano Lett. 10: 3101–3105.

[7] Lindman, S., Lynch, I., Thulin, E., Nilsson, H., Dawson, K.A., Linse, S. (2007): Systematic investigation of the thermodynamics of HSA adsorption to N-iso-Propylacrylamide/N-tert-Butylacrylamide copolymer nanoparticles effects of particle size and hydrophobicity. Nano Lett. 7: 914–920.

[8] Zhang, G., Ma, Y. (2013): Mechanistic and conformational studies on the interaction of food dye amaranth with human serum albumin by multispectroscopic methods. Food Chem. 136: 442–449.

[9] Mpountoukas, P., Pantazaki, A., Kostareli, E., Christodoulou, P., Kareli, D., Poliliou, S., Mourelatos, C., Lambropoulou, V., Lialiaris, T. (2010): Cytogenetic evaluation and DNA interaction studies of the food colorants amaranth, erythrosine and tartrazine. Food Chem. Toxicol. 48: 2934–2944.

[10] Ishidate Jr., M., Sofuni, T., Yoshikawa, K., Hayashi, M., Nohmi, T., Sawada, M., Matsuoka, A. (1984): Primary mutagenicity screening of food additives currently used in Japan. Food Chem. Toxicol. 22: 623–636.

[11] Basu, A., Suresh Kumar, G. (2014): Study on the interaction of the toxic food additive carmoisine with serum albumins: a microcalorimetric investigation. J.Hazard. Mater. 273: 200–206.

[12] Nevado, J.J.B., Cabanillas, C.G., Salcedo, A.M.C. (1995): Simultaneous spectrophotometric determination of three food dyes by using the first derivative of ratio spectra. Talanta 42: 2043–2051.

[13] Perutz, M.F., Rossmann, M.G., Cullis, A.F., Muirhead, H., Will, G., North, A.C.T. (1960): Structure of haemoglobin: a three-dimensional Fourier synthesis at 5.5-Å. resolution, obtained by X-ray analysis. Nature 185: 416–422.
[14] Perutz, M.F. (1963): X-ray analysis of hemoglobin. Science 140: 863–869.
[15] Lu, D., Zhao, X., Zhao, Y., Zhang, B., Zhang, B., Geng, M., Liu, R. (2011): Binding of sudan II and sudan IV to bovine serum album: comparison studies. Food Chem.Toxicol. 49: 3158–3164.
[16] Peng, W., Ding, F., Peng, Y.-K., Sun, Y. (2014): Molecular recognition of malachite green by hemoglobin and their specific interactions: insights from in silico docking and molecular spectroscopy. Mol. Biosyst. 10: 138–148.
[17] Chatterjee, S., Suresh Kumar, G. (2014): Targeting the heme proteins hemoglobin and myoglobin by janus green blue and study of the dye–protein association by spectroscopy and calorimetry. RSC Adv. 4: 42706–42715.
[18] Mandal, P., Bardhan, M., Ganguly, T. (2010): A detailed spectroscopic study on the interaction of Rhodamine 6G with human hemoglobin. Journal of Photochemistry and Photobiology B: Biology 99: 78–86.
[19] Wang, M., Zhang, H., Tang, B. P. (2010): The interaction of C.I. acid red 27 with human hemoglobin in solution. Journal of Photochemistry and Photobiology B: Biology 100: 76–83.
[20] Bhavsar, M.D., Amiji, M.M. (2007): Gastrointestinal distribution and in vivo gene transfection studies with nanoparticles-in microsphere oral system (NiMOS). J. Control Release 119: 339–348.
[21] Sun, W., Zhang, N., Li, X. (2012): Release mechanism studies on TFu nanoparticles-in-microparticles system, Colloids Surf B Biointerfaces 95: 115–120.
[22] Galeano, E., Martinez, A. *(*2007): Antimicrobial activity of marine sponges from Uraba Gulf. Colombian caribean region. J. Med Mycol. 17: 21-24.
[23] Manmode, A.S., Sakarkar, D., Mahajan, N. (2009): Nanoparticles Tremendous Therapeutic Potential: a Review. Int. J. Pharm. Tech. Res. 1(4):1020-1027.
[24] Larkin, P. (2011): Infrared and Raman Spectroscopy Principles and Spectral Interpretation. Elsevier Inc.
[25] Wo´zniak, M., Ratajczak, Z., Szentner, K., Kwa´sniewska, P., Mazela, B., (2015): Propolis and organosilanes in wood protection. Part I: FTIR analysis and biological tests, Annals of Warsaw University of Life Sciences – SGGW Forestry and Wood Technology. 91: 218–224.
[26] Benesi, H.A., Hildebrand, J.H. (1949): A spectrophotometric investigation of the interaction of iodine with aromatic hydrocarbons. J. Am. Chem. Soc. 71: 2703–2707.
[27] Venkatesh rao, S., Manoharan, P.T. (2004): Conformational changes monitored by fluorescence study on reconstituted hemoglobins. Spectrochim. Acta A. 60: 2523–2526.
[28] Mueser, T.C., Rogers, P.H., Arnone, A. (2000): Interface sliding as illustrated by the multiple quaternary structures of liganded hemoglobin. Biochemistry 39: 15353–15364.
[29] Alpert, D.M., Jameson, Weber, G. (1980): Tryptophan emission from human hemoglobin and its isolated subunits. Photochem. Photobiol. 31: 1–4.
[30] Lakowicz, J.R. (1999): Principles of Fluorescence Spectroscopy. Plenum Press. New York.
[31] Lakowicz, J.R. (2006): Principles of Fluorescence Spectroscopy. third ed. Springer Science + Business Media. New York. 63–606
[32] Xie, M.X., Xu, X.Y., Wang, Y.D., (2005): Interaction between hesperetin and human serum albumin revealed by spectroscopic methods. Biochim. Biophys. Acta. 1724: 215–224.
[33] Lloyd, J.B.F. (1971): Synchronized excitation of fluorescence emission spectra. Nat. Phys. Sci. 231: 64–65.
[34] Miller, J.N. (1979): Recent advances in molecular luminescence analysis. Proc. Anal. Div. Chem. Soc. 16: 203–208.

[35] Kapanidis, A.N., Laurence, T.A., Lee, N.K., Margeat, E., Kong, X., Weiss, S. (2005): Alternating laser excitation of single molecules. Acc. Chem. Res. 38: 523–533.
[36] Mallick, A., Haldar, B., Chattopadhyay, N., (2005): Spectroscopic investigation on the interaction of ICT probe 3-Acetyl-4-oxo-6,7-dihydro-12H Indolo-[2,3-a] quinolizine with serum albumins. J. Phys. Chem. B 109: 14683–14690.
[37] Jash, C., Suresh Kumar, G. (2014): Binding of alkaloids berberine, palmatine and coralyne to lysozyme: a combined structural and thermodynamic study. RSC Adv. 4: 12514–12525.
[38] Valeur, B., Brochon, J.C. (2001): New Trends in Fluorescence Spectroscopy. Springer-Verlag, Berlin.
[39] Basu, A., Suresh Kumar, G. (2016): Multispectroscopic and calorimetric studies on the binding of the food colorant tartrazine with human hemoglobin. J. Hazard. Mater. 318: 468-476.